R-92L and R-92W Mutations in Cardiac Troponin T Lead to Distinct Energetic Phenotypes in Intact Mouse Hearts

Huamei He,*† Maryam M. Javadpour,* Farhana Latif,†§ Jil C. Tardiff,†§ and Joanne S. Ingwall*
*NMR Laboratory for Physiological Chemistry, Division of Cardiovascular Medicine, Department of Medicine, Brigham and Women's Hospital and Harvard Medical School, Boston, Massachusetts 02115; and †Department of Physiology and Biophysics and §Division of Cardiology, Department of Medicine, Albert Einstein College of Medicine Bronx, New York 10461

ABSTRACT It is now known that the flexibility of the troponin T (TnT) tail determines thin filament conformation and hence cross-bridge cycling properties, expanding the classic structural role of TnT to a dynamic role regulating sarcomere function. Here, using transgenic mice bearing R-92W and R-92L missense mutations in cardiac TnT known to alter the flexibility of the TnT tropomyosin-binding domain, we found mutation-specific differences in the cost of contraction at the whole heart level. Compared to age- and gender-matched sibling hearts, mutant hearts demonstrate greater ATP utilization measured using ^{31}P NMR spectroscopy as decreases in [ATP] and [PCr] and $|\Delta G_{\sim ATP}|$ at all workloads and profound systolic and diastolic dysfunction at all energetic states. R-92W hearts showed more severe energetic abnormalities and greater contractile dysfunction than R-92L hearts. The cost of increasing contraction was abnormally high when [Ca^{2+}] was used to increase work in mutant hearts but was normalized with supply of the β-adrenergic agonist dobutamine. These results show that R-92L and R-92W mutations in the TM-binding domain of cardiac TnT alter thin filament structure and flexibility sufficiently to cause severe defects in both whole heart energetics and contractile performance, and that the magnitude of these changes is mutation specific.

INTRODUCTION

Muscle contraction occurs when the thick filament protein myosin interacts with specific domains of the thin filament protein actin, coupling the energy released from ATP hydrolysis ($\Delta G_{\sim ATP}$) by myosin to force generation. Availability of these myosin-binding domains of actin for cross-bridge formation depends on the interaction of the thin filament regulatory proteins tropomyosin (TM) and the three troponin (Tn) subunits, TnT, TnC, and TnI. Cross-bridge cycling depends on both Ca^{2+}-dependent activation of TnC and Ca^{2+}-independent conformational changes in TnT. The tail portion of TnT binds to TM where the two TM polypeptide chains overlap, changing the flexibility of the thin filament (1). This determines the affinity of the TnT-TM complex for actin, which in turn determines the availability of myosin-binding domains on actin for cross-bridge formation. Experiments using model systems have shown that changing the TnT-TM interaction by deleting the TnT tail domain alters actomyosin ATPase activity, in vitro motility of actin-TM filaments on myosin heads, and cooperativity of myosin subfragment-1 binding to thin filaments (2,3). Thus, in addition to playing the classical structural role in the thin filament, TnT also plays a crucial dynamic role in the regulation of the contractile cycle and ATP utilization by the sarcomere.

Missense mutations in the tail portion of cardiac TnT (cTnT) discovered by association with the cardiac disease familial hypertrophic cardiomyopathy (FHC) have been shown to lead to a cardiac phenotype characterized by contractile dysfunction with modest or no left ventricular hypertrophy and early sudden death (4). R-92 is a ''hotspot'', with many FHC-associated missense mutations, each leading to a unique progression of disease. R-92 is located in the elongated tail domain of cTnT adjacent to the critical site of overlap of the TM monomers. Our group has previously found that substituting glutamine (Q) for arginine (R) at residue 92 of cTnT in transgenic mouse hearts increased the cost of contraction assessed as decreased free energy available from ATP hydrolysis, $|\Delta G_{\sim ATP}|$, and abolished the ability of the heart to increase contractile performance (5). This study showed that changes in the structure of the TM-binding domain of cTnT caused by the R-92Q missense mutation led to increased cost of contraction at the whole heart level, but it has yet to be tested whether this is unique to this mutation or whether all FHC-associated mutations in this region of the thin filament alter sarcomere dynamics and function leading to an increased cost of contraction.

Recently, using molecular dynamics simulations, our group found that substituting either tryptophan (W) or leucine (L) for R at residue 92 of cTnT alters the flexibility and dynamics of the cTnT domain that binds to TM and that each mutation yields a unique average conformation (6). Replacing 50% of wildtype cTnT with cTnT bearing either the R-92W or R-92L mutation in mice using genetic tools allowed us to define the consequences of the changes in cTnT tail flexibility caused by these single amino acid replacements (6). Both mutant hearts demonstrated ventricular and cellular

Submitted February 25, 2007, and accepted for publication May 10, 2007.

Address reprint requests to Joanne S. Ingwall, PhD, NMR Laboratory for Physiological Chemistry, 221 Longwood Ave, 247 BLI, Boston, MA 02115. Tel.: 617-732-6994; Fax: 617-732-6990; E-mail: jingwall@rics.bwh.harvard.edu.

Humei He's present address is The Children's Hospital, Harvard Medical School, Boston MA 02115.

Editor: Cristobal G. dos Remedios.

0006-3495/07/09/1834/11 $2.00

doi: 10.1529/biophysj.107.107557

remodeling and contractile dysfunction, but the changes for R-92W hearts were more severe than for R-92L hearts. Thus, each mutation led to unique peptide conformation and dynamics and produced unique cardiac phenotypes in mice. What is not known is whether the cost of contraction increases in mouse hearts bearing either the R-92W or R-92L mutation in cTnT, and, if so, whether the magnitude of the change is mutation specific. Here, using these well-characterized mice, we test the hypotheses that replacing R-92 in the TM-binding domain of cTnT with either R-92W or R-92L leads to sufficiently large perturbations in thin filament structure and sarcomere function to change sarcomere energetics at the whole heart level and that the magnitude of the changes is mutation specific. We defined the energetic state of the isolated perfused heart using the noninvasive tool of ^{31}P NMR spectroscopy while simultaneously measuring contractile performance. We found that hearts bearing R-92W and R-92L mutations have distinct energetic phenotypes.

METHODS

Characteristics of R-92 mouse hearts

Twenty-three-week-old male mice bearing *c-myc*–tagged murine cTnT with either the R-92L or R-92W cTnT mutation were generated as described (6); sibling mice without mutation were used as nontransgenic (nTG) controls. Each animal was genotyped by PCR-amplified tail DNA and restriction enzyme digestion to confirm the presence or absence of mutation codon. To confirm that the hearts studied here demonstrated the same gross morphologic properties as hearts from R-92 mutant mice described by us previously, body weight (BW), heart weight (HW), atrial mass, left ventricular (LV) mass, the ratio of HW to BW, LV chamber volume, LV chamber radius and wall thickness were determined (Table 1). BW was comparable among R-92W, R-92L and nTG mice. HW, the ratio of HW to BW, LV mass and LV wall thickness for R-92L mice were larger than those in nTG mice, and much larger than those for R-92W mice. HW, the ratio of HW to BW, LV mass and LV chamber volume in R-92W mice were smaller than those for nTG mice. Atrial mass for both R-92L and R-92W hearts were larger than that for nTG hearts. Thus, in agreement with our previous report (6), transgenic hearts used for this study bearing the R-92L mutation in cTnT were ~19% larger than nTG hearts whereas hearts bearing the R-92W mutation were ~10% smaller. Animals were maintained in accordance with National Institutes of Health guidelines for the care and use of laboratory animals. The experimental protocol was approved by the Standing Committee on Animals of Harvard Medical Area and followed current National Institutes of Health and American Physiologic Society guidelines.

TABLE 1 Characteristics of nTG, R-92L, and R-92W mice

	nTG	R-92L	R-92W
n	16	10	12
BW (g)	27.2 ± 1.0	28.6 ± 1.3	27.4 ± 1.4
HW (mg)	115 ± 4	137 ± 4†	104 ± 4*‡
HW/BW (mg g^{-1})	4.3 ± 0.1	4.8 ± 0.2*	3.8 ± 0.1*‡
Atrial mass (mg)	7.2 ± 0.6	18.1 ± 1.1†	15.9 ± 1.5†
LV mass (mg)	86 ± 2	99 ± 2*	69 ± 2†‡
LV chamber volume (μl)	18 ± 1	11 ± 1†	11 ± 1†
LV chamber radius (mm)	1.6 ± 0.1	1.4 ± 0.1†	1.4 ± 0.1†
LV wall thickness (mm)	1.2 ± 0.1	1.6 ± 0.1†	1.2 ± 0.1‡
Protein (mg/mg wet weight)	0.207 ± 0.003	0.213 ± 0.007	0.203 ± 0.006

*$p < 0.05$.
$^{\dagger}p < 0.01$ vs. nTG.
$^{\ddagger}p < 0.05$ vs. R = 92L.

Isolated perfused heart preparation and measurement of isovolumic contractile performance

Hearts were isolated and perfused in the Langendorff mode in a 10-mm glass NMR tube as described (7). Briefly, the chest was opened; the heart was excised and arrested in ice-cold buffer, and connected via the aorta to the perfusion cannula. Retrograde perfusion was carried out at a constant coronary perfusion pressure of 75 mmHg at 37°C with phosphate-free Krebs-Henseleit (KH) buffer containing (in mM): NaCl, 118; KCl, 5.3; $CaCl_2$, 2.5; $MgSO_4$, 1.2; EDTA, 0.5; $NaHCO_3$, 25; and glucose, 10; equilibrated with 95% O_2/5% CO_2, yielding a pH of 7.4. Right ventricular drainage was accomplished by incision of the pulmonary artery. Effluent from the Thebesian veins was drained by a thin polyethylene tube (PE-10) pierced through the apex of the left ventricle. A water-filled balloon custom-made of polyvinylchloride film connected to a pressure transducer (Statham P23Db, Gould Statham, Medical Provision Department, Oxnard, CA) was used for continuous recording of left ventricular systolic pressure (LVSP) and heart rate (HR) (7). The balloon matched the size of the ventricular cavity and was inflated to set LV end diastolic pressure (EDP) to ~10 mmHg; the balloon volume was then held constant. Isovolumic contractile performance data were collected online at a sampling rate of 200 Hz using a commercially available data acquisition system (MacLab; ADInstruments, Milford, MA). LV developed pressure (DevP; the difference between LVSP and EDP), the minimum and maximum values within a beat of the first derivative of LV pressure (+dP/dt and −dP/dt), and rate-pressure product (RPP, i.e., product of DevP and HR) were calculated offline. Coronary flow rate was measured by collecting coronary sinus effluent through the suction tube (ml min^{-1}).

Experimental protocols

Three protocols were used. In the first protocol, hearts (six each) from R-92L, R-92W, and sibling nTG mice were perfused with KH buffer containing 2 mM free Ca^{2+} (total 2.5 mM); HR was not paced. After a 20-min stabilization period, isovolumic contractile performance and ^{31}P NMR spectroscopy were measured simultaneously for 24 min. Hearts were then perfused with KH buffer containing 3.5 mM free Ca^{2+} (total 4.0 mM). After steady state was reached (~4 min), cardiac function and ^{31}P NMR spectroscopy were measured simultaneously for another 24 min. In the second protocol, HR was paced at 420 beats min^{-1} (bpm) using monophasic square-wave pulses delivered from a stimulator (model S88; Grass Instrument, Quincy, MA) through salt-bridge pacing wires consisting of PE-90 tubing filled with 4 M KCl in 2% agarose. Isovolumic contractile performance and ^{31}P NMR spectroscopy were measured simultaneously when hearts were perfused with KH buffer containing 2 and then 3.5 mM free Ca^{2+}, each for 24 min. In the third protocol, hearts from three R-92L, five R-92W, and six nTG mice were perfused with KH buffer containing 2 mM free Ca^{2+} and paced at 420 bpm. After a 20-min stabilization period, isovolumic contractile performance and ^{31}P NMR spectroscopy were measured simultaneously for 24 min. Hearts were then studied unpaced at high workload achieved by infusing dobutamine (final concentration 300 nM) by a side-tube. After steady state was reached, cardiac function and ^{31}P NMR spectroscopy were measured simultaneously for another 24 min. Based on preliminary experiments, the doses of Ca^{2+} and dobutamine used produced >90% of the maximum contractile responses. At the end of each of these experiments, hearts were removed from the perfusion apparatus, blotted, and weighed.

The atria were removed, and the ventricles were rapidly frozen in liquid N_2 and stored at −80°C for subsequent biochemical assays.

^{31}P NMR spectroscopy and calculation of metabolite concentrations

Isolated perfused hearts were placed in a 10-mm glass NMR sample tube and inserted into a custom-made $^{1}H/^{31}P$ double-tuned probe situated in an 89-mm bore 9.4-T superconducting magnet. To improve homogeneity of the NMR-sensitive volume, the perfusate level was adjusted so that the heart was submerged in buffer. ^{31}P NMR spectra were obtained without proton decoupling by using a 60° flip angle, 15-μs pulse width, 2.4-s recycle time, 6,000-Hz sweep width and 2K data points at 161.94 MHz on a GE-400 wide-bore Omega spectrometer (General Electric, Fremont, CA). Single spectra were collected during 12-min periods and consisted of data averaged from 312 free induction decays. Spectra were analyzed using 20-Hz exponential multiplication and zero and first-order phase corrections. The resonance areas corresponding to ATP, phosphocreatine (PCr), and inorganic phosphate (Pi) were quantified using Bayesian Analysis software (G.L. Bretthorst, Washington University, St. Louis, MO). Bayesian Analysis software uses a direct statistical analysis of the free induction decay amplitudes, which corresponds to the resonance areas (8). By comparing the amplitude under the peaks from fully relaxed (recycle time 15 s) and those of partially saturated (recycle time 2.4 s) spectra, the correction factors for saturation were calculated for ATP (1.0), PCr (1.2), and Pi (1.15).

To determine the cytosolic concentration of ATP, the absolute resonance amplitude corresponding to [γ-P]ATP in the ^{31}P NMR spectra during baseline perfusion was normalized by heart weight. Since the Lowry protein content (which minimizes detection of extracellular matrix protein and thereby approximates myocyte protein) was indistinguishable among three groups (Table 1), we make the assumption that the ratio of intracellular volume to cardiac mass of 0.48 μL/mg wet weight was the same for all hearts (7). In this case, amplitude units/g wet weight is directly proportional to the absolute intracellular concentrations. The value of 10 mmol L^{-1} for [ATP] for nTG mouse myocardium (9) was used to calibrate the [γ-P]ATP peak amplitude of the ^{31}P NMR spectrum obtained during baseline perfusion period. The mean of the amplitude of the [γ-P]ATP resonances was used for this calculation. Changes in ATP, PCr, and Pi concentrations during the protocols were calculated by multiplying the ratio of their resonance peak amplitude to the mean amplitude of the [γ-P]ATP peaks from the initial baseline spectrum by 10 mmol L^{-1}. Intracellular pH was determined by comparing the differences in the chemical shifts of Pi and PCr resonances in each spectrum to values from a standard curve; the chemical shift of Pi but not PCr varies with pH.

Cytosolic free [ADP] was calculated using the equilibrium expression for the creatine kinase reaction and values for ATP, PCr, creatine (see below), and H^+ concentrations obtained by NMR spectroscopy and biochemical assay: $[ADP] = ([ATP][free\ creatine]) / ([PCr][H^+]K_{eq})$, where K_{eq} is 1.66×10^9 M^{-1} for a $[Mg^{2+}]$ of 1.0 mM. The free energy released by ATP hydrolysis ($\Delta G_{\sim ATP}$) drives the ATPase reactions in the cell. Although $\Delta G_{\sim ATP}$ is a negative value, the change in free energy state due to release of $\Delta G_{\sim ATP}$ by ATP hydrolysis is a positive value. Here we describe changes in $\Delta G_{\sim ATP}$ in absolute values, denoted as $|\Delta G_{\sim ATP}|$, and calculated as $|\Delta G_{\sim ATP}|$ (kJ/mol) $= |\Delta G_o + RT \ln ([ADP][Pi] / [ATP])|$, where ΔG_o (–30.5 kJ/mol) is the value of $\Delta G_{\sim ATP}$ under standard conditions of molarity, temperature, pH, and $[Mg^{2+}]$, R is the gas constant (8.3 J/mol K), and T is the temperature in degrees Kelvin.

Biochemical measurements

Five to ten mg of ventricular tissue was homogenized for 10 s at 4°C in potassium phosphate buffer containing 1 mmol L^{-1} EDTA and 1 mmol L^{-1} β-mercaptoethanol, pH 7.4 (final concentration of 5 mg wet weight ml^{-1}). Aliquots were removed for assay of protein (10) and total creatine (11) contents.

Statistical analysis

All results are expressed as mean ± SE. Differences among the three groups were compared by one-way factorial ANOVA followed by t-test, and changes between baseline and high workload were compared by repeated-measure ANOVA. Linear relationships were fitted using least squares method. All statistical analyses were performed with STATVIEW (Brain Power, Calabasas, CA), and a value of $p < 0.05$ was considered significant.

RESULTS

To determine whether alterations in thin filament structure caused by substituting either L or W for R at position 92 of cTnT are sufficient to change whole heart energetics at baseline and the cost of increasing contraction in a mutation-specific manner, we used ^{31}P NMR spectroscopy to simultaneously measure [ATP], [PCr], and [Pi] and indices of systolic and diastolic performance in isolated hearts of age- and sex-matched sibling R-92L, R-92W, and nTG mice. We used three experimental protocols: 1), unpaced at baseline conditions and during perfusion with high $[Ca^{2+}]$ to increase contractile performance; 2), paced both at baseline and during perfusion with high $[Ca^{2+}]$; and 3), paced at baseline and then unpaced during perfusion with dobutamine. Figs. 1 *A* and *B* shows representative ^{31}P NMR spectra obtained from nTG, R-92L and R-92W hearts acquired during baseline perfusion and then at high workload in response to either high $[Ca^{2+}]$ or dobutamine. Mean values for [ATP], [PCr], [Pi], and [ADP] are shown in Table 2. Fig. 2 *A* and *B* shows corresponding representative tracings of isovolumic contractile performance. Mean values for HR, DevP, +dP/dt and −dP/dt are shown graphically in Fig. 3; values for all indices of systolic and diastolic function are given in Table 1 of the Supplementary Materials.

R-92L and R-92W cTnT hearts have lower free energy of ATP hydrolysis and lower contractile performance at baseline

^{31}P NMR spectra obtained from nTG hearts during baseline perfusion showed typical high ratios of PCr to ATP (>1.8) and PCr to Pi (>6). Compared to nTG hearts, R-92L hearts had lower [ATP] (by ~16%) and [PCr] (by ~22%), and higher [Pi] (~1.4-fold) and [ADP] (~1.3-fold). R-92W hearts demonstrated even greater differences: [ATP] (~21%), [PCr] (~29%), [Pi] (1.9-fold higher), and [ADP] (1.6-fold higher). Intracellular pH was similar in all hearts and averaged 7.12. The decreases in [PCr] in R-92L and R-92W hearts were not due to decreases in total [creatine], which were not different (27, 26, and 26 mmol L^{-1} for nTG, R-92L, and R-92W hearts, respectively). Instead, the decrease in [PCr] is due to increased ATP utilization.

Changes in [ATP], [ADP], and [Pi] can be expressed as a single parameter, the free energy of ATP hydrolysis, $\Delta G_{\sim ATP}$. This value represents the chemical driving force for the ATPase reactions and describes the energy state of the cell.

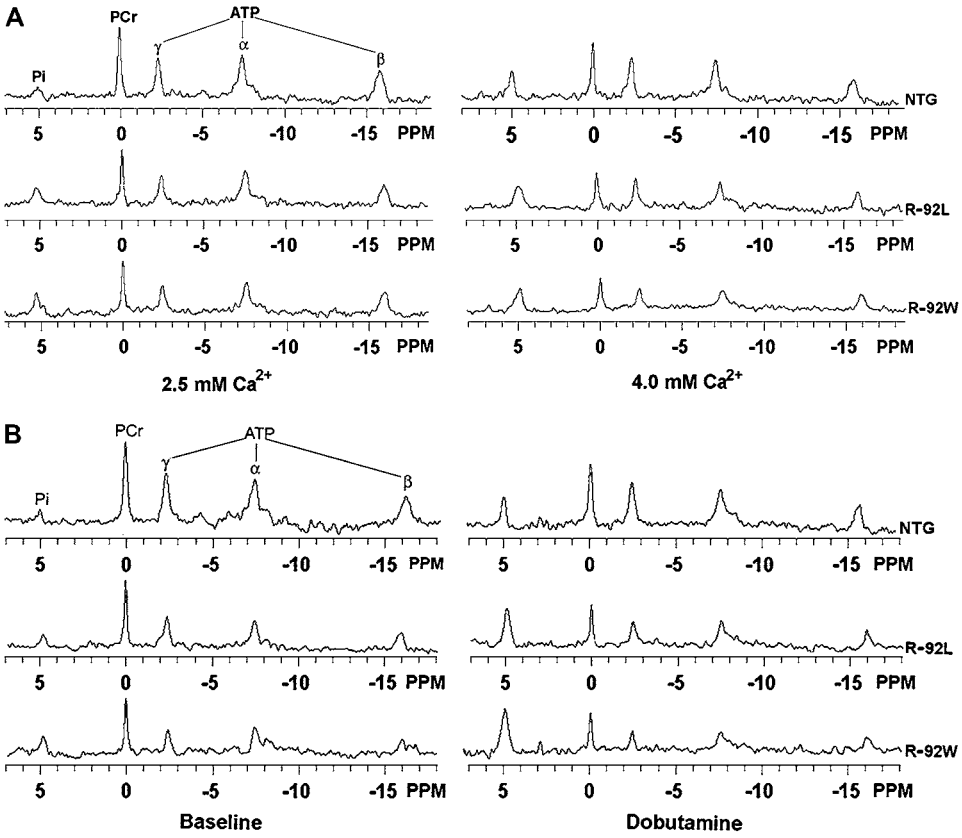

FIGURE 1 Representative ^{31}P NMR spectra from three to six 23-week-old nTG (*upper panels*), R-92L (*middle panels*) and R-92W (*lower panels*) mutant hearts at baseline (*left*) and at high workload (*right*) to 4 mM Ca^{2+} (*A*) and in response to 300 nM dobutamine (*B*). Resonance areas from left to right correspond to Pi, PCr, and $\gamma-$, α, and β-phosphates of ATP. At baseline, R-92L hearts showed higher Pi resonance area, but lower PCr and ATP resonance areas than did nTG hearts, R-92W hearts demonstrated even greater differences compared with R-92L hearts. nTG hearts exhibited an increase in Pi resonance area, and decreases in PCr resonance area, but similar ATP resonance area at high workload in both *A* and *B* compared with at baseline. R-92L and R-92W hearts showed even greater changes in Pi, PCr and ATP resonance areas compared with at baseline as well as nTG hearts at high workload. PPM, parts per million.

For well-oxygenated beating mammalian hearts, $|\Delta G_{\sim ATP}|$ is typically ~60 kJ mol^{-1} at low work states and ~54–56 kJ mol^{-1} at high work states. As expected, $|\Delta G_{\sim ATP}|$ for the nTG hearts at low work states is ~60 kJ mol^{-1}. Compared to nTG hearts, $|\Delta G_{\sim ATP}|$ is ~2.4 kJ mol^{-1} lower for R-92L hearts and even lower, by ~3.9 kJ mol^{-1}, for R-92W hearts (Fig. 4).

During baseline perfusion of unpaced nTG hearts, LVSP was ~122 mmHg, the ratio of +dP/dt to –dP/dt was >1, and RPP was ~40 × 10^3 mmHg min^{-1}, all values typical for

TABLE 2 Energetics of hearts bearing cTnT mutations at baseline and at high workload in response to 4 mM Ca^{2+} or 300 nM dobutamine when not paced or paced at 420 bpm (n = 3-6)

	nTG			R-92L			R-92W		
	Unpaced	Paced	Dobutamine	Unpaced	Paced	Dobutamine	Unpaced	Paced	Dobutamine
Baseline									
Pi (mM)	2.7 ± 0.2	3.2 ± 0.2	2.8 ± 0.1	4.0 ± 0.2†	4.5 ± 0.2†	4.5 ± 0.6†	5.1 ± 0.3†‡	6.0 ± 0.2†‡	6.8 ± 0.3†¶
PCr (mM)	18.2 ± 0.3	18.2 ± 0.4	19.5 ± 0.1	14.1 ± 0.3†	14.3 ± 0.4†	15.4 ± 0.7†	12.9 ± 0.5†‡	12.5 ± 0.3†‡	13.6 ± 0.4†‡
ATP (mM)	10.0 ± 0.3	9.9 ± 0.3	9.9 ± 0.3	8.7 ± 0.2†	8.1 ± 0.2†	8.2 ± 0.5†	7.9 ± 0.2†‡	7.5 ± 0.3†	7.5 ± 0.5†
ADP (μM)	35 ± 2	35 ± 3	35 ± 1	55 ± 2*	50 ± 2*	44 ± 3†	63 ± 2†	62 ± 2†‡	55 ± 4†‡
High workload									
Pi (mM)	6.0 ± 0.2$^{\parallel}$	6.4 ± 0.3$^{\parallel}$	8.4 ± 0.4$^{\parallel}$	7.8 ± 0.2$^{\dagger\parallel}$	7.9 ± 0.1$^{\dagger\parallel}$	11.0 ± 0.5$^{\dagger\parallel}$	9.0 ± 0.2$^{\dagger\ddagger\parallel}$	9.0 ± 0.2$^{\dagger\ddagger\parallel}$	13.1 ± 0.6$^{\dagger\ddagger\parallel}$
PCr (mM)	13.5 ± 0.2$^{\parallel}$	13.3 ± 0.6$^{\parallel}$	13.8 ± 0.1$^{\parallel}$	10.5 ± 0.3$^{\dagger\parallel}$	10.6 ± 0.3$^{\dagger\parallel}$	10.2 ± 0.5$^{\dagger\parallel}$	8.5 ± 0.2$^{\dagger\ddagger\parallel}$	8.6 ± 0.3$^{\dagger\ddagger\parallel}$	7.9 ± 0.4$^{\dagger\ddagger\parallel}$
ATP (mM)	9.8 ± 0.3	9.6 ± 0.4	9.6 ± 0.5	7.7 ± 0.1$^{\dagger\parallel}$	7.6 ± 0.3†	7.5 ± 0.4†	6.9 ± 0.2†‡§	6.6 ± 0.3*‡§	6.4 ± 0.2†‡§
ADP (μM)	71 ± 3$^{\parallel}$	73 ± 3$^{\parallel}$	78 ± 1$^{\parallel}$	89 ± 6*$^{\parallel}$	83 ± 7 *$^{\parallel}$	87 ± 3*$^{\parallel}$	109 ± 9*$^{\ddagger\parallel}$	100 ± 6$^{\dagger\ddagger\parallel}$	117 ± 6$^{\dagger\ddagger\parallel}$

Intracelluar pH in all hearts at baseline and high workload showed no differences, ranging from 7.08 to 7.13. $\Delta G_{\sim ATP}$ is presented in Fig. 4. M, mol L^{-1}.
*$p < 0.05$.
$^{\dagger}p < 0.01$ vs. nTG.
$^{\ddagger}p < 0.05$.
$^{\P}p < 0.01$ vs. R-92L.
$^{\S}p < 0.05$.
$^{\parallel}p < 0.01$ vs. baseline.

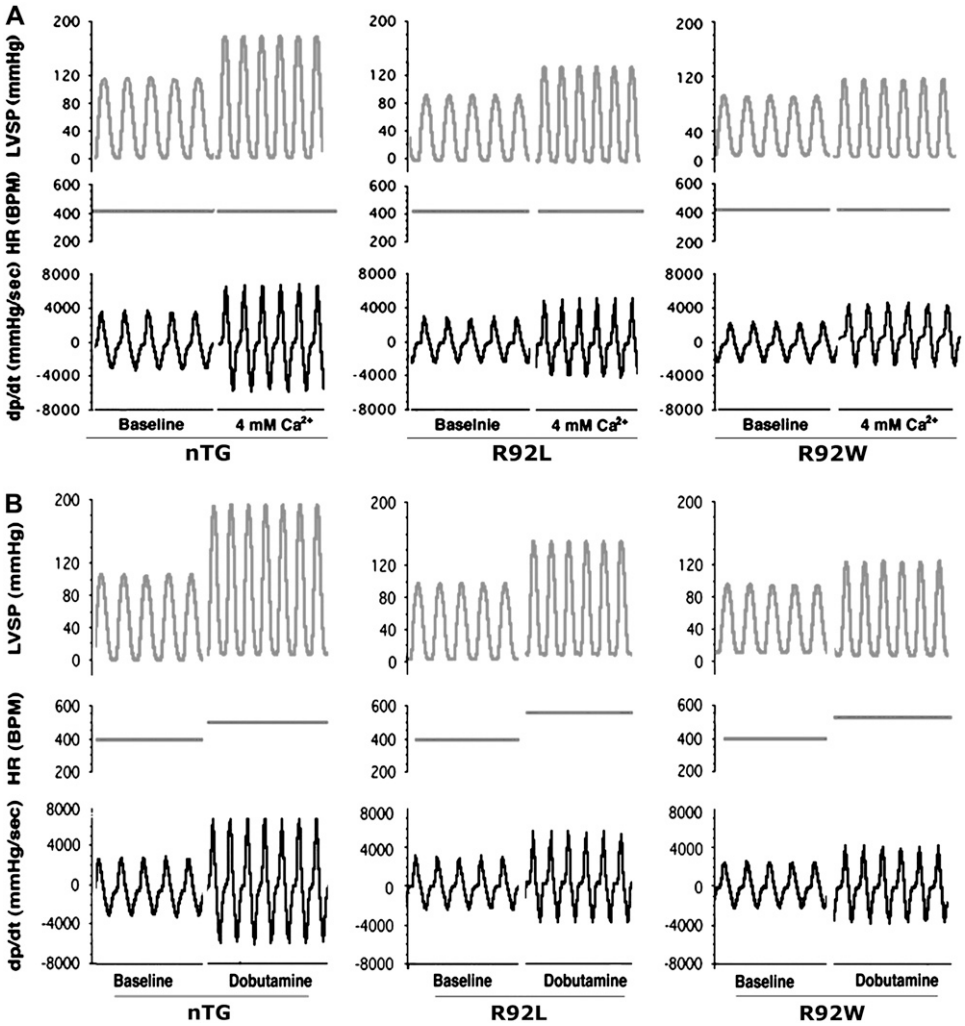

FIGURE 2 Representative tracings of isovolumic contractile performance from three to six 23-week-old nTG (*left column*), R-92L (*middle column*) and R-92W (*right column*) mutant hearts at baseline (*left*) and at high workload (*right*) in response to 4 mM Ca^{2+} (A) and to 300 nM dobutamine (B). The tracings from the top to the bottom correspond to LVSP, HR, the minimum and maximum values within a beat of the first derivative of LV pressure (+dP/dt and −dP/dt). R-92L hearts showed the decreases in LVSP, +dp/dt and −dp/dt at baseline, and decreased response to 4 mM Ca^{2+} and to 300 nM dobutamine compared with nTG hearts. R-92W hearts demonstrated even greater decrease in LVSP, +dp/dt and −dp/dt at baseline and worse response to 4 mM Ca^{2+} and to 300 nM dobutamine compared toR-92L hearts. The heart was paced at 420 bpm at baseline and at high workload in response to 4 mM Ca^{2+}. The heart was not paced when challenged with 300 nM dobutamine.

mouse hearts isolated and perfused in the Langendorff mode. Increasing HR by ~18% by pacing at 420 bpm led to a corresponding increase of ~15% in RPP with no change in other indices of contractile performance. Whether R-92 mutant mouse hearts were paced or unpaced, indices of both systolic and diastolic contractile performance differed from those for nTG hearts. Despite the larger size of the R-92L hearts, all indices of systolic performance were lower for R-92L hearts than for nTG hearts. Indices of systolic performance for the smaller R-92W hearts were even lower. RPP, the index of contractile performance that takes into account changes in HR, LVSP, and EDP, was ~16% lower for R-92L hearts and ~26% lower for R-92W hearts compared to nTG hearts. The rate of relaxation was also lower for both R-92L and R-92W hearts, with the slowest rate found for R-92W hearts (−22%).

Thus, for identical conditions of perfusate composition, perfusion pressure, coronary flow and temperature, and independent of pacing status, hearts bearing R-92 cTnT missense mutations have lower free energy of ATP hydrolysis, and the driving force for ATPase reactions for R-92W hearts is even lower than for R-92L hearts. Systolic performance and the rate of relaxation were lower than for nTG hearts, with the lowest values found for R-92W hearts.

R-92L and R-92W cTnT hearts demonstrate decreased contractile reserve

We then compared the ability of the mutant hearts to abruptly increase contractile performance, i.e., recruit their contractile reserve, using two different agents that increase contractile performance, high perfusate [Ca^{2+}] and dobutamine, an agent that increases HR as well as force of contraction.

When perfusate [Ca^{2+}] was increased from 2.5 to 4 mM, all hearts responded by increasing systolic and diastolic performance. However, the mutation-specific differences in contractile performance observed at baseline were not only preserved, but the decreases in systolic and diastolic performance observed for the R-92 mutant hearts became even larger at high work states. Compared to nTG hearts, all indices of systolic performance at high workloads for unpaced hearts were ~25% lower for R-92L hearts and ~40% lower

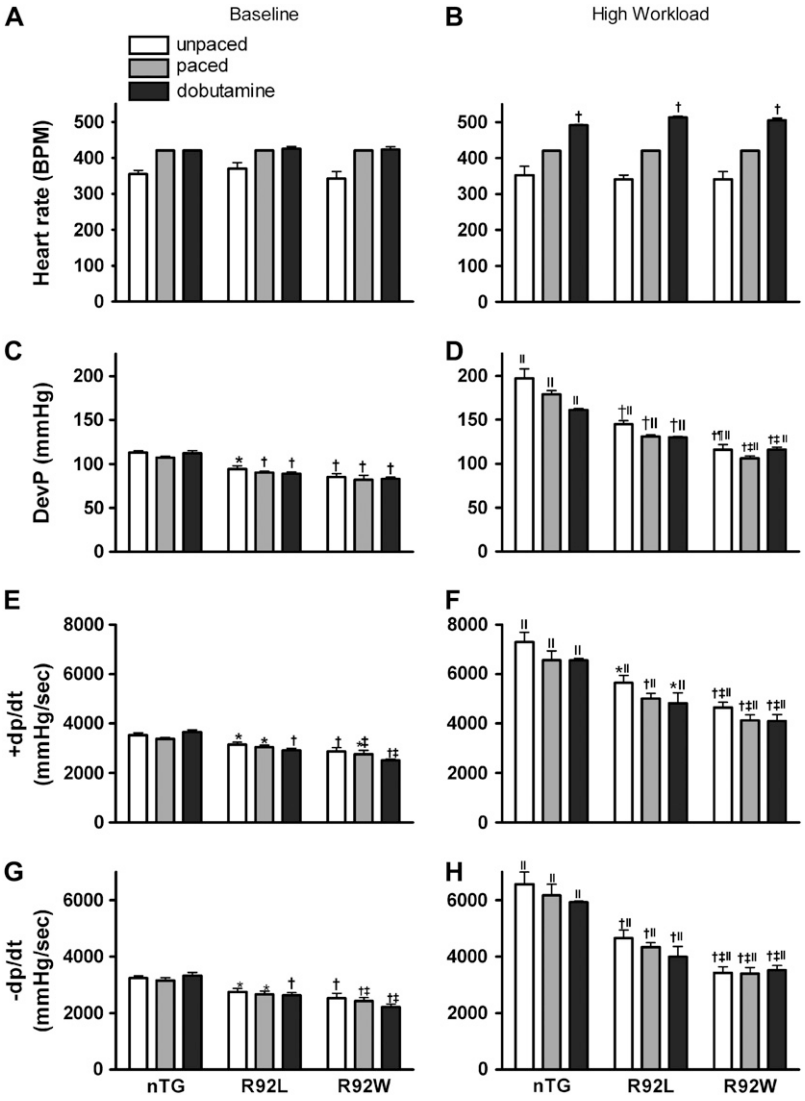

FIGURE 3 Contractile performance of hearts bearing R-92 cTnT mutations under baseline perfusion conditions (*left columns*) and at high workload (*right columns*) in response to either 4 mM Ca^{2+} when not paced or paced at 420 bpm or 300 nM Dobutamine. Data shown are mean ± SE, n = 3–6. For the pairs from top to bottom: (*A*) heart rate at baseline and (*B*) heart rate at high workload; (*C*) developed pressure (difference between left ventricular systolic pressure and end diastolic pressure) at baseline and (*D*) developed pressure at high workload; (*E*) +dp/dt at baseline, and (*F*) +dp/dt at high workload; (*G*) −dp/dt at baseline, and (*H*) −dp/dt at high workload. $*p < 0.05$; $^{\dagger}p < 0.01$ vs nTG; $^{\ddagger}p < 0.05$; $^{\|}p < 0.01$ vs. baseline.

for R-92W hearts. EDP did not increase for nTG hearts, but increased by ~5 mmHg for both R-92L and R-92W hearts. The rate of relaxation increased by ~2.0 for nTG, ~1.7 for R-92L, and only ~1.3 times for R-92W hearts. A similar pattern was observed for paced hearts. Thus, in response to an abrupt increase in work caused by increasing external $[Ca^{2+}]$, paced and unpaced mutant hearts demonstrated both systolic and diastolic dysfunction, and R-92W hearts exhibited even greater systolic and diastolic dysfunction than R-92L hearts.

The normal physiological response to supplying high $[Ca^{2+}]$ is to increase DevP without a change in HR whereas in response to dobutamine both HR and DevP increase. However, since the increase in DevP with dobutamine is less than with high $[Ca^{2+}]$, RPP is only slightly higher with dobutamine than in response to high $[Ca^{2+}]$. This response was observed here for nTG hearts, but the mutant hearts demonstrated greater sensitivity to dobutamine. Compared to nTG hearts, mutant hearts had greater increases in HR, and although DevP was always lower compared to nTG hearts, RPP for mutant hearts increased more with dobutamine than with high $[Ca^{2+}]$. The increases in RPP for the three challenges (high $[Ca^{2+}]$ unpaced, high $[Ca^{2+}]$ paced, and dobutamine) were 28, 30, and 32 × 10^3 mmHg min^{-1}, respectively for nTG hearts; 15, 17, and 29 × 10^3 mmHg min^{-1} for R-92L hearts; and 10, 10, and 24 × 10^3 mmHg min^{-1} for R-92W hearts. These results show that both mutant hearts fail to recruit normal levels of contractile reserve in response to high perfusate $[Ca^{2+}]$ and that β-adrenergic stimulation partially rescues their contractile reserve assessed as the increase in RPP. The increase in EDP in mutant hearts was also less with dobutamine; however, DevP and the rates of tension development and relaxation were the same with high $[Ca^{2+}]$ and dobutamine. Importantly, the rescue with dobutamine is more complete for R-92L hearts than for R-92W hearts.

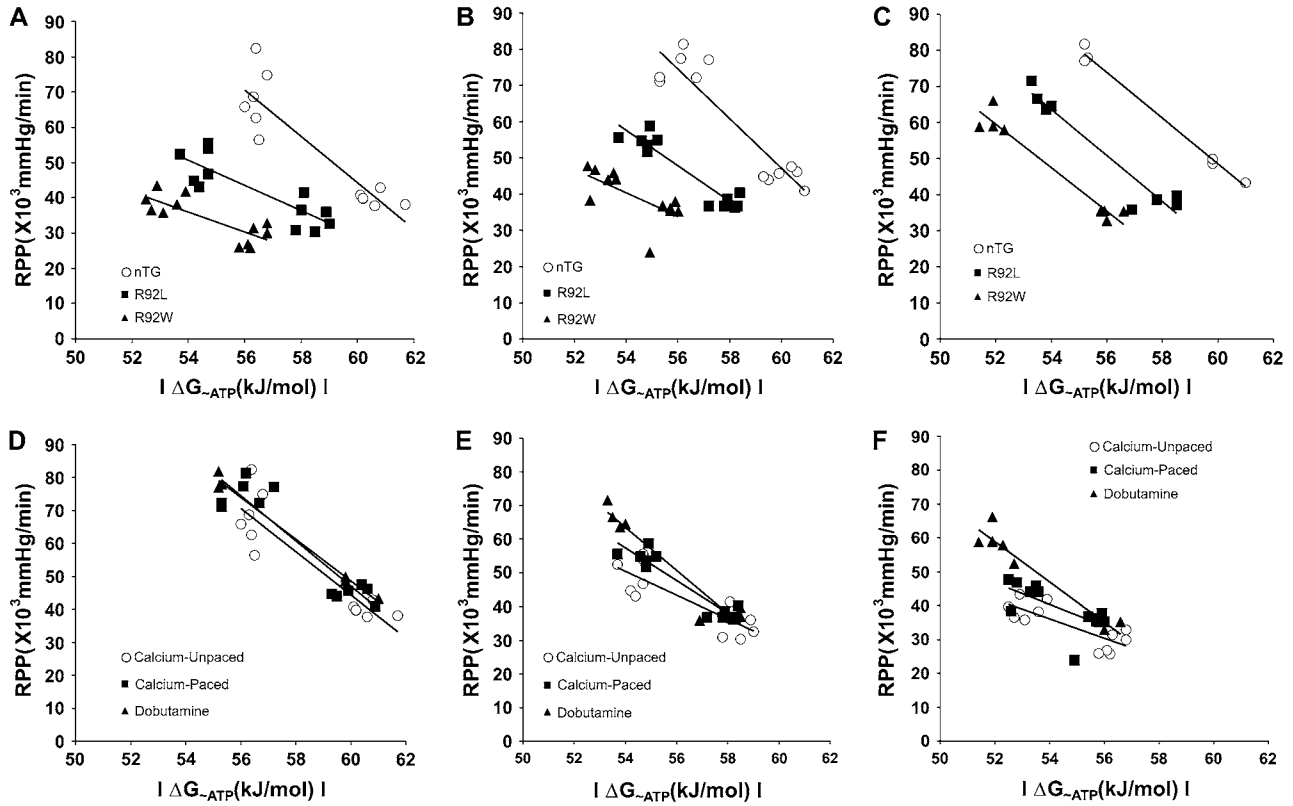

FIGURE 4 Plots of the relationship between RPP and $|\Delta G_{\sim ATP}|$ for nTG, R-92L and R-92W hearts under the three protocols: unpaced +4 mM Ca^{2+}, paced +4 mM Ca^{2+} and paced + 300 nM dobutamine. RPP was from supplementary Table 1, $|\Delta G_{\sim ATP}|$ was calculated from the data in Table 2. The equations, the inverse of the slopes, the assessment of goodness for the linear fits of data by group and by protocol are summarized in Table 3. (*A*) hearts from nTG (*open circles*), R-92L (*solid squares*), and R-92W (*solid triangles*) were not paced both at baseline and high workload in response to 4 mM Ca^{2+}; (*B*) hearts from nTG (*open circles*), R-92L (*solid squares*) and R-92W (*solid triangles*) were paced both at baseline and high workload in response to 4 mM Ca^{2+}; (*C*) hearts from nTG (*open circles*), R-92L (*solid squares*), and R-92W (*solid triangles*) were paced at baseline but not paced at high workload in response to 300 nM dobutamine; (*D*) nTG hearts were perfused by three protocols: unpaced-high calcium (*open circles*), paced-high calcium (*solid squares*) and dobutamine (*solid triangles*); (*E*) R-92L hearts were perfused by three protocols: unpaced-high calcium (*open circles*), paced-high calcium (*solid squares*), and dobutamine (*solid triangles*); (*F*) R-92W hearts were perfused by three protocols: unpaced-high calcium (*open circles*), paced-high calcium (*solid squares*), and dobutamine (*solid triangles*). The number of trials is three to six.

Mutation-specific differences in energetics persist at high work states

As expected based on previous studies of mouse and other rodent hearts comparing baseline and inotropic challenge (12), increasing contractile performance led to a fall in [PCr] and increases in [Pi] and [ADP] with either unchanged or only slightly decreased [ATP] in all hearts. This pattern demonstrates increased energy utilization due to increased workload at the whole heart level; i.e., the creatine kinase reaction supplies sufficient phosphoryl groups to closely match ATP utilization at high workload by hydrolyzing PCr. Unlike the mutation-specific differences in contractile performance found in response to high $[Ca^{2+}]$ and to dobutamine, changes in values of [PCr], [Pi], and $|\Delta G_{\sim ATP}|$ for the same physiological challenge were similar for mutant and nTG hearts. Consistent with greater energetic differences found for R-92W hearts at baseline, only R-92W hearts demonstrated a fall in [ATP] at all high work states. Thus the differences in energetics observed at baseline among nTG and mutant hearts persisted at high workload, but were not exacerbated at high work states.

The cost of increasing contraction in response to high $[Ca^{2+}]$ and to dobutamine differed for the mutant hearts but not for the nTG hearts

To assess the energetic cost of increasing isovolumic contractile performance as opposed to defining baseline energetics, the relationships between RPP versus $|\Delta G_{\sim ATP}|$ were defined for nTG, R-92L, and R-92W hearts for the three protocols. The three upper panels in Fig. 4 allow comparisons among the three groups of hearts by experimental protocol; the lower panels show the same results making comparisons among the protocols for each type of heart. Note that, in this representation, an increase in RPP results in lower $|\Delta G_{\sim ATP}|$, i.e., the energy state of the heart becomes

lower as a result of increasing work. Table 3 presents the linear fits of the data by group and protocol; the inverse of the slope represents the energetic cost of increasing contraction at the whole heart level.

For nTG hearts, the linear fits for RPP versus $|\Delta G_{\sim ATP}|$ for the three protocols are indistinguishable, and the cost of increasing contraction for each challenge is the same, ~0.15 kJ $mol^{-1}/10^3$ mmHg min^{-1} (Fig. 4 *D*). The patterns for the R-92L and R-92W hearts are strikingly different. Regardless of the agent used to elicit an increase in contractile performance, data for R-92W hearts fall to the left of data for R-92L hearts, which in turn fall to the left of nTG hearts, showing mutation-specific differences that are independent of work state (Fig. 4, *A–C*). It can be seen that for any constant RPP (see Fig. 4, *A–C*), values for $|\Delta G_{\sim ATP}|$ for mutant hearts are lower than for nTG hearts, demonstrating increased cost of contraction that is mutation specific. For example, for RPP of 40×10^3 mmHg min^{-1}, a typical baseline value for nTG hearts, values for $|\Delta G_{\sim ATP}|$ are 61, 57, and 55 kJ mol^{-1} for nTG, R-92L, and R-92W paced hearts, respectively (Fig. 4 *B*). Comparable differences are found at all work states and for all protocols. Conversely, for the same constant $|\Delta G_{\sim ATP}|$, mutant hearts have lower RPP, demonstrating profound systolic dysfunction for the same energetic state. For example, for $|\Delta G_{\sim ATP}|$ of 56 kJ mol^{-1} for paced hearts challenged with high $[Ca^{2+}]$ (Fig. 4 *B*), RPP generated by R-92L hearts is ~61% of nTG RPP values, and R-92W hearts generate only ~48% of nTG RPP values.

When high $[Ca^{2+}]$ was used to increase contractile performance for unpaced hearts, the cost of increasing contraction (inverse of the slopes of the linear fits shown in Fig. 4 and given in Table 3) was nearly twice as high for R-92L as for nTG hearts (0.28 vs. 0.15 kJ $mol^{-1}/10^3$ mmHg min^{-1}), and the cost was even higher for R-92W hearts (0.38 kJ $mol^{-1}/10^3$ mmHg min^{-1}). Pacing improved (i.e., lowered) the cost of increasing RPP, especially for R-92L hearts, but still remained high. When dobutamine was used as the challenge to increase contractile performance, a different pattern was observed. Now, despite the persistent genotype-specific leftward shifts for the relationships between RPP and $|\Delta G_{\sim ATP}|$, the cost of increasing contraction was the same for all hearts (0.16 kJ $mol^{-1}/10^3$ mmHg min^{-1}). These results suggest that contractile reserve, but not the intrinsic energetic state, of myocardium from R-92 cTnT mutant mice can be rescued, at least in part, by β-adrenergic stimulation. These conclusions are the same even if the cost of increasing contraction is adjusted for the small differences in [ATP] observed for the three groups.

TABLE 3 Linear regression parameters of RPP against $|\Delta G_{\sim ATP}|$ for nTG, R-92 mutant hearts for three protocols: unpaced with high $[Ca^{2+}]$, paced with high $[Ca^{2+}]$, and with dobutamine

	Unpaced (r) −1/m	Paced (r) −1/m	Dobutamine (r) −1/m
nTG	Y = −6.5x + 440 (0.90) 0.15	Y = −6.8x + 430 (0.92) 0.15	Y = −6.3x + 430 (0.99) 0.16
R-92L	Y = −3.6x + 240 (0.85) 0.28	Y = −4.9x + 320 (0.94) 0.20	Y = −6.4x + 410 (0.96) 0.16
R-92W	Y = −2.8x + 190 (0.80) 0.36	Y = −3.2x + 220 (0.66) 0.31	Y = −5.9x + 370 (0.97) 0.17

(r), assessment of goodness of fit; 1/m, inverse of slope, kJ/10^3 mmHg min^{-1}.

DISCUSSION

Changes in peptide dynamics due to R-92 missense mutations in cTnT lead to unique cardiac phenotypes

Using molecular dynamic simulations to study the stability and conformation of the cTnT peptide containing residues 70–170, our group previously reported that the presence of either R-92L or R-92W mutation altered the flexibility around a hinge formed by residues 104–108, decreasing helical stability of the peptides. It was also found that the two mutations differed in terms of motion quantified as the radius of gyration, with little motion for the WT peptide and marked oscillations for R-92L; motion for the R-92W peptide was intermediate. Thus, each missense mutation at R-92 in cTnT produced unique peptide dynamics. The consequences of these changes in cTnT peptide dynamics for the functioning of the intact sarcomere and for the whole heart cannot be predicted. Here, using well characterized transgenic mouse models, we report that replacing R-92 with either R-92L or R-92W in cTnT produces unique energetic and contractile phenotypes in intact beating hearts.

These observations that the cost of contraction and contractile performance at all work states for R-92L and R-92W cTnT hearts are severely impaired suggest that the structural and dynamic changes in the thin filament caused by R-92 missense mutations in the TM-binding domain of TnT disrupt the normal transmission of the Ca^{2+}-signaling cascade. This could occur directly within the thin filament by disrupting the transmission from the Ca^{2+}-sensor TnC to the TnT-TM complex (13). It could also occur at the sarcomere level if the entire sarcomere is structurally altered by the cTnT mutation sufficiently to disrupt the titin-obscurin linkage between the sarcomere and sarcoplasmic reticulum (14). Although the details of how this occurs are not known, our study shows that single amino acid replacements at R-92 in cTnT alter peptide structure and dynamics in the thin filament in such a way that contractile performance is impaired and cost of contraction is increased at the whole heart level. Importantly, this is the case independent of the presence or absence of neurohumoral stimulation, changes in heart rate, and the nature of the inotropic challenge, showing that contractile dysfunction is due to the presence of the R-92 missense mutations in cTnT (50% replacement). It is noteworthy that mice bearing the FHC-associated missense mutation in the TnT-binding site of TM at residue 180 (E-180G) also demonstrate contractile dysfunction (15); the energetic state

was not defined. Taken together, these results show that altered peptide dynamics in this region of the thin filament leads to contractile dysfunction at the whole heart level.

Results reported here show that substituting R at residue 92 in cTnT with either L or W also increase ATP utilization. Whereas previous experiments using isolated skinned fibers from R-92L and R-92W cTnT hearts failed to show increased tension cost (16,17), it is important to note that the original R-92Q cTnT fiber studies did not show an effect on tension cost until >90% mutant cTnT replacement was achieved. In contrast, our earlier whole heart experiments using whole hearts in which 50% R-92 was replaced with R-92Q clearly showed increased tension cost (5). Thus, the threshold for these two types of experiments differs (16,17). Our studies were made using 23-week-old (adult) mice. During the life of the animal it is reasonable to expect that altered sarcomere structure and dynamics would lead to secondary molecular alterations beyond the sarcomere. Important for our studies, ATP supply pathways assessed as V_{max} of key mitochondrial, glycolytic, and phosphotransfer enzymes, are normal (not shown), supporting our conclusion that the increased tension cost is due primarily to ATP utilization.

R-92 cTnT mutations lead to increased cost of contraction at all work loads

The conformational changes that occur in thick and thin filament proteins during the contractile cycle are energetically unfavorable and must be coupled to the hydrolysis of ATP to proceed. The chemical driving force for ATPase reactions is quantitatively expressed as the free energy of ATP hydrolysis, $\Delta G_{\sim ATP}$. Free energy available from ATP hydrolysis is calculated as a constant value for ATP hydrolysis under standard conditions of temperature and molarity corrected for actual concentrations of ATP and its products of hydrolysis, ADP and Pi. Here we observe that hearts bearing R-92W and R-92L missense mutations in cTnT have lower [ATP] and [PCr], higher [ADP] and [Pi], and consequently lower $|\Delta G_{\sim ATP}|$ than age- and gender-matched nTG sibling hearts. The changes are mutation specific, with R-92W demonstrating greater differences than R-92L compared to nTG hearts. This is the case for both baseline conditions and high workloads, and is independent of the maneuver used to increase work: pacing, high $[Ca^{2+}]$ or dobutamine. These changes in energy metabolites and in $|\Delta G_{\sim ATP}|$ demonstrate greater ATP utilization and show that altered sarcomere dynamics and function caused by the missense mutations in cTnT are sufficient to increase ATP utilization determined at the whole heart level. The observation that [ATP] as well as [PCr] is lower than for normal heart shows that ATP utilization exceeds the ability of the ATP-supply pathways to maintain a constant [ATP]. Since work states achieved by supplying dobutamine to the isolated heart mimic work states typically observed in vivo, the mutant mice have a remarkable ability to adapt to energy-poor conditions.

The differences in $|\Delta G_{\sim ATP}|$ of 4–6 kJ mol^{-1} observed here for R-92L and R-92W cTnT hearts compared to nTG hearts at both low and high work states, are unexpectedly large. For comparison, the maximum fall in $|\Delta G_{\sim ATP}|$ observed for the normal intact heart during abrupt increases in work is typically 6 kJ mol^{-1}. Replacing native $\alpha\alpha$- with $\beta\beta$-myosin heavy chain in mouse hearts changed $|\Delta G_{\sim ATP}|$ by only 2–3 kJ mol^{-1} (12), and, for all hearts studied here, the further increase in RPP elicited by using dobutamine instead of high $[Ca^{2+}]$ led to a fall in $|\Delta G_{\sim ATP}|$ of only ~1 kJ mol^{-1} change. One predicted consequence of such large deficits in $|\Delta G_{\sim ATP}|$ for R-92 mutant sarcomeres would be to limit the ability of the sarcomere to increase force development. Studying intact hearts containing 50% mutant cTnT we observed large deficits in force development measured as DevP and in the rates of tension development and relaxation, and reduced ability to increase work upon acute challenge. ATPase reactions can be controlled thermodynamically if the chemical driving force for a particular reaction falls to its threshold. Values of the free energy available from ATP hydrolysis found here for the mutant hearts were close to the thermodynamic limit for the sarcoplasmic reticular Ca^{2+}-ATPase but not myosin ATPase (18).

High cytosolic concentrations of the end products of ATP hydrolysis are sufficient to alter cross-bridge cooperativity and Ca^{2+}-sensitivity leading to reduced force development and slower rates of relaxation. Recently Homsher et al. (19) suggested that either slower ADP release or slower ATP binding to myosin reduces shortening velocity. We suggest that this could occur in hearts if [ADP] increased. For both skeletal and cardiac muscle, when all other variables are controlled, increases in [ADP] have also been shown to result in greater diastolic dysfunction (20). The R-92 cTnT mutant hearts studied here have lower [ATP] and higher [ADP] and demonstrated decreased DevP and slower rates of tension development and relaxation at all work states. Whereas local regeneration of ATP in the sarcomere occurs by phosphotransferase reactions associated with myofibrillar proteins, such as creatine kinase and adenylate kinase, it seems likely that the cytosolic concentrations of ADP and ATP determined here for the whole heart reflect changes in local concentrations as well. It is noteworthy that R-92W cTnT hearts, with more contractile dysfunction than R-92L cTnT hearts, had lower [ATP] and higher [ADP], suffered loss of [ATP] at high work states, and had lower $|\Delta G_{\sim ATP}|$ than R-92L cTnT hearts. These changes in [ATP] and [ADP] may contribute to the contractile dysfunction observed in the mutant hearts.

β-Adrenergic stimulation normalizes the cost of increasing contraction in R-92 cTnT mutant hearts by increasing the rate of contraction, not tension development

The large improvement in contractile reserve measured as an increase in RPP and hence normalization in the cost of

increasing contraction in response to dobutamine compared to high [Ca^{2+}] was unexpected. This cannot be explained by an improved energetic state because $|\Delta G_{\sim ATP}|$ fell as RPP increased with dobutamine supply, nor can it be explained by changes in intracellular pH affecting sarcomere function, as it was unchanged. Rather it is due to increased ATP turnover in response to increased HR. RPP, an index of isovolumic contractile performance, takes into account changes in rate of contraction as well as tension development (DevP). The relationship between RPP and $|\Delta G_{\sim ATP}|$ show stepwise increases in efficiency as HR increased by ~70 bpm going from unpaced to paced conditions and as HR increased another 70–80 bpm with dobutamine (Fig. 4, *E* and *F*). Importantly, despite increases in HR, defects in DevP and rates of tension development and relaxation persisted, consistent with impaired sarcomere function due to altered cTnT structure and dynamics.

Increased cost of contraction is a common end point of FHC-associated mutations of sarcomeric proteins

Each FHC-associated missense mutation at R-92 in the N-terminal tail domain of cTnT leads to a clinically distinct cardiomyopathy. Our group has previously found that substituting glutamine (Q) for arginine (R) at residue 92 of cTnT increased the cost of contraction at the whole heart level (5). Increases in the cost of contraction have also been observed in mouse hearts bearing the FHC-associated R-403Q mutation in the actin-binding loop of myosin (21), and would explain the observations that PCr to ATP ratio is lower in hearts of patients with FHC due to mutations in many different sarcomere proteins (22). Taken together, these results suggest the hypothesis that a common consequence of the different FHC-associated mutations in sarcomeric proteins is an increased cost of cardiac contraction. The results presented here using well characterized mice bearing mutations R-92L and R-92W in cTnT provide a direct test of this hypothesis. Our results show that substitution at R-92 in the TM-binding domain of TnT with L (this study), W (this study) or Q (5) increases the cost of contraction. Importantly, they show that the increase in the cost of contraction is mutation specific: the rank order for lower $|\Delta G_{\sim ATP}|$ is L > W > Q and directly corresponds to decreased contractile performance (L > W > Q). These results provide a structural-energetic basis for the unique cardiac phenotypes observed in patients with contractile protein-associated FHC.

CONCLUSIONS

It is now known that the flexibility of the TnT tail determines thin filament conformation and hence cross-bridge cycling properties, further expanding the classic structural role of TnT to a dynamic role regulating sarcomere function (1,2). Changes in cTnT flexibility and dynamics have been found to differ for each of three FHC-associated amino acid substitutions at R-92 (6), suggesting a potential biophysical mechanism for the mutation-specific phenotypes observed in patients with cTnT-associated FHC. To directly model this system, we used mouse hearts bearing different missense mutations at R-92 of cTnT known to alter the flexibility of the cTnT TM-binding domain and found mutation-specific differences in the cost of contraction at the whole heart level, profound systolic and diastolic contractile dysfunction at all energetic states, and impaired contractile reserve that was partially rescued by supplying the β-adrenoceptor-agonist dobutamine. In all cases, R-92W cTnT hearts demonstrated greater dysfunction than R-92L hearts. These findings suggest a direct link between mutation-specific changes in the flexibility and dynamics of the cTnT N-terminal tail domain caused by the R-92L and R-92W mutations and unique cardiac clinical phenotypes that are characteristic of FHC.

SUPPLEMENTARY MATERIAL

To view all of the supplemental files associated with this article, visit www.biophysj.org.

We thank Dr. S. Schwartz for helpful discussions.

This work was supported by grants from the National Institutes of Health.

REFERENCES

1. Palm, T., S. Graboski, S. E. Hitchcock-DeGregori, and N. J. Greenfield. 2001. Disease-causing mutations in cardiac troponin T: identification of a critical tropomyosin-binding region. *Biophys. J.* 81:2827–2837.
2. Maytum, R., M. A. Geeves, and S. S. Lehrer. 2002. A modulatory role for the troponin T tail domain in thin filament regulation. *J. Biol. Chem.* 277:29774–29780.
3. Tobacman, L. S., M. Nihli, C. Butters, M. Heller, V. Hatch, R. Craig, W. Lehman, and E. Homsher. 2002. The troponin tail domain promotes a conformational state of the thin filament that suppresses myosin activity. *J. Biol. Chem.* 277:27636–27642.
4. Tardiff, J. C. 2005. Sarcomeric proteins and familial hypertrophic cardiomyopathy: linking mutations in structural proteins to complex cardiovascular phenotypes. *Heart Fail. Rev.* 10:237–248.
5. Javadpour, M. M., J. C. Tardiff, I. Pinz, and J. S. Ingwall. 2003. Decreased energetics in murine hearts bearing the R92Q mutation in cardiac troponin T. *J. Clin. Invest.* 112:768–775.
6. Ertz-Berger, B. R., H. He, C. Dowell, S. M. Factor, T. E. Haim, S. Nunez, S. D. Schwartz, J. S. Ingwall, and J. C. Tardiff. 2005. Changes in the chemical and dynamic properties of cardiac troponin T cause discrete cardiomyopathies in transgenic mice. *Proc. Natl. Acad. Sci. USA.* 102:18219–18224.
7. Saupe, K. W., M. Spindler, R. Tian, and J. S. Ingwall. 1998. Impaired cardiac energetics in mice lacking muscle-specific isoenzymes of creatine kinase. *Circ. Res.* 82:898–907.
8. Bretthorst, G. L., J. J. Kotyk, and J. J. Ackerman. 1989. 31P NMR Bayesian spectral analysis of rat brain in vivo. *Magn. Reson. Med.* 9: 282–287.
9. Saupe, K. W., M. Spindler, J. C. Hopkins, W. Shen, and J. S. Ingwall. 2000. Kinetic, thermodynamic, and developmental consequences of deleting creatine kinase isoenzymes from the heart. Reaction kinetics of the creatine kinase isoenzymes in the intact heart. *J. Biol. Chem.* 275: 19742–19746.

10. Lowry, O. H., N. J. Rosenbrough, A. L. Farr, and R. J. Randall. 1951. Protein measurement with the folin phenol reagent. *J. Biol. Chem.* 193: H729–H744.

11. Kammermeier, H. 1973. Microassay of free and total creatine from tissue extracts by combination of chromatography and fluorometric methods. *Anal. Biochem.* 56:341–345.

12. Hoyer, K., M. Krenz, J. Robbins, and J. S. Ingwall. 2007. Shifts in the myosin heavy chain isozymes in the mouse heart result in increased energy efficiency. *J. Mol. Cell. Cardiol.* 42:214–221.

13. Solaro, J. R., and J. Van Eyk. 1996. Altered interactions among thin filament proteins modulate cardiac function. *J. Mol. Cell. Cardiol.* 28:217–230.

14. Kontrogianni-Konstantopoulos, A., D. H. Catino, J. C. Strong, S. Sutter, A. B. Borisov, D. W. Pumplin, M. W. Russell, and R. J. Bloch. 2006. Obscurin modulates the assembly and organization of sarcomeres and the sarcoplasmic reticulum. *FASEB J.* 20:2102–2111.

15. Michele, D. E., C. A. Gomez, K. E. Hong, M. V. Westfall, and J. M. Metzger. 2002. Cardiac dysfunction in hypertrophic cardiomyopathy mutant tropomyosin mice is transgene-dependent, hypertrophy-independent, and improved by beta-blockade. *Circ. Res.* 91:255–262.

16. Chandra, M., M. L. Tschirgi, and J. C. Tardiff. 2005. Increase in tension-dependent ATP consumption induced by cardiac troponin T mutation. *Am. J. Physiol. Heart Circ. Physiol.* 289:H2112–H2119.

17. Montgomery, D. E., J. C. Tardiff, and M. Chandra. 2001. 2001. Cardiac troponin T mutations: correlation between the type of mutation and the nature of myofilament dysfunction in transgenic mice. *J. Physiol.* 536: 583–592.

18. Ingwall, J. S. 2002. The chemistry of the ATPase reaction. *In* ATP and the Heart. B. Swynghedauw, editor. Kluwer Academic Publishers, Norwell, MA. 21–37.

19. Homsher, E., M. Nili, I. Y. Chen, and L. S. Tobacman. 2003. Regulatory proteins alter nucleotide binding to acto-myosin of sliding filaments in motility assays. *Biophys. J.* 85:1046–1052.

20. Tian, R., M. E. Christe, M. Spindler, J. C. Hopkins, J. M. Halow, S. A. Camacho, and J. S. Ingwall. 1997. Role of MgADP in the development of diastolic dysfunction in the intact beating rat heart. *J. Clin. Invest.* 99:745–751.

21. Spindler, M., K. W. Saupe, M. E. Christe, H. L. Sweeney, C. E. Seidman, J. G. Seidman, and J. S. Ingwall. 1998. Diastolic dysfunction and altered energetics in the alphaMHC403/+ mouse model of familial hypertrophic cardiomyopathy. *J. Clin. Invest.* 101:1775–1783.

22. Crilley, J. G., E. A. Boehm, E. Blair, B. Rajagopalan, A. M. Blamire, P. Styles, W. J. McKenna, I. Ostman-Smith, K. Clarke, and H. Watkins. 2003. Hypertrophic cardiomyopathy due to sarcomeric gene mutations is characterized by impaired energy metabolism irrespective of the degree of hypertrophy. *J. Am. Coll. Cardiol.* 41:1776–1782.